3b2 v7 DSRII : 927 -
pp.1–23 (col.fig.: NIL)
PROD.TYPE: COM
ED: SHIV;BRR
PAGN: ANANTH SCAN: ROOPA

PERGAMON

Deep-Sea Research II 0 (2001) 1–23

DEEP-SEA RESEARCH
PART II

www.elsevier.com/locate/dsr2

Upper ocean export of particulate organic carbon and biogenic silica in the Southern Ocean along 170°W

K.O. Buesseler[a,*], L. Ball[a], J. Andrews[a], J.K. Cochran[b], D.J. Hirschberg[b], M.P. Bacon[a], A. Fleer[a], M. Brzezinski[c]

[a] *Department of Marine Chemistry and Geochemistry, Woods Hole Oceanographic Institution, Clark Building 447, Woods Hole, MA 02543-1541, USA*

[b] *Marine Sciences Research Center, State University of New York, Stony Brook, NY 11794, USA*

[c] *Department of Ecology, Evolution and Marine Biology, University of California, Santa Barbara, Santa Barbara, CA 93106, USA*

Received 21 April 2000; received in revised form 11 September 2000; accepted 6 October 2000

Abstract

Upper-ocean fluxes of particulate organic carbon (POC) and biogenic silica (bSi) are calculated from four US JGOFS cruises along 170°W using a thorium-234 based approach. Both POC and bSi fluxes exhibit large variability vs. latitude during the seasonal progression of diatom dominated blooms. POC fluxes at 100 m of up to 50 mmol C m^{-2} d^{-1} are found late in the bloom, and farthest south near the Ross Sea Gyre. Biogenic Si fluxes also peak late in the bloom as high as 15 mmol Si m^{-2} d^{-1}, but this flux peak occurs at a different latitude, just south of the Antarctic Polar Front (APF), which is centered around 60°S along this cruise track. The ratios of both POC and bSi export relative to their production rates are large, suggesting an efficient biological pump at these latitudes. The highest relative bSi/POC flux ratios at 100 m are found just south of the APF, coincident with a bSi/POC flux peak seen in 1000 m traps during this same program by Deep-Sea Research II (submitted). These data suggest that efficient export at these latitudes can support the high accumulation rates of bSi found in the sediments under and south of the APF, despite the generally low biomass and productivity levels in this region. © 2001 Published by Elsevier Science Ltd.

1. Introduction

The US Joint Global Ocean Flux Study (JGOFS) organized a series of cruises in the western Pacific sector of the Antarctic Ocean to follow the progression of the austral spring/summer bloom across the Polar Frontal region. The Southern Ocean was chosen as a key region to study

*Corresponding author. Tel.: +1-508-289-2309; fax: +1-508-457-2193.
E-mail address: kbuesseler@whoi.edu (K.O. Buesseler).

0967-0645/01/$ - see front matter © 2001 Published by Elsevier Science Ltd.
PII: S0967-0645(01)00089-3

because of its potential influence on climate through carbon uptake and sequestration (Sarmiento and Toggweiler, 1984; Kumar et al., 1995). The large reservoir of unutilized macronutrients in the surface waters of the Antarctic Circumpolar Current is sufficient to significantly impact atmospheric carbon dioxide levels if conditions stimulating their use were to arise (Sarmiento and Toggweiler, 1984). The area to the south of the Antarctic Convergence is also the single most important sedimentary sink for biogenic silica (bSi) in the global ocean (DeMaster, 1981; Treguer et al., 1995). Much of the accumulation of opal in Southern Ocean sediments occurs in a band of nearly circumglobal siliceous oozes, whose northern edge lies beneath the Antarctic Polar Front (APF). On glacial time scales, large variations in the magnitude and position of C and Si burial are seen in the sedimentary record, and a simple link between surface process and the sediment record is often assumed (DeMaster et al., 1991; Mortlock et al., 1991). However, surface production and export are often decoupled, and the controls on export appear to have important temporal and regional variability that are not directly proportional to local primary productivity levels (e.g., Buesseler, 1998). The factors controlling the rate and magnitude of the export of particulate carbon, bSi and other nutrient elements from the upper ocean remain key uncertainties in studies and models that predict significant regulation of global carbon cycling in the Southern Ocean.

One of the goals of the US JGOFS Antarctic Environment and Southern Ocean Process Study (AESOPS) was to examine in detail the relationships between C and Si uptake and export. A long-standing issue in the Southern Ocean is how the sediment accumulation rates of organic C and bSi in particular can be so high, despite relatively short growth cycles and low productivity rates. At issue is the efficiency of the biological pump and whether seasonally elevated export fluxes on sinking particles and minimal remineralization in the water column can support the high accumulation of bSi found in the sediments below the APF zone, or whether enhanced preservation in the sediments need be invoked.

We report here the first estimates of the upper-ocean export fluxes of particulate organic carbon (POC) and bSi along a transect at 170°W in the Southern Ocean. The results are derived from thorium-234 ($t_{1/2} = 24.1$ d), a naturally occurring radionuclide that has been widely used as a tracer of particle export in the upper ocean. Both steady state and non-steady state modeling are used to estimate ^{234}Th fluxes from the measured ^{234}Th profiles. These flux data are then converted to particulate fluxes of POC and bSi using the measured ratios of C and Si to ^{234}Th on large particles (>70 μm) collected at depth during the same cruises. The data allow for a seasonal estimate of particulate export at 1000 m across a transect along 170°W between 55°S and 70°S. The overall accuracy of these flux estimates is evaluated by comparing the ^{234}Th-based export fluxes to the rates of Si and C uptake (Brzezinski et al., 2000a; Hiscock et al., 2000) and to the export of these materials at 1000 m determined from sediment traps (Honjo et al., 2000). The study enables us to make a regional estimate of particulate export to improve our understanding of the strength of the biological pump in the Southern Ocean in particular, and the rates and controls on export in general.

2. Sampling and analyses

2.1. Sampling sites

Thorium-234, POC and bSi samples were collected during four cruises on the *R/V Revelle* as part of the US JGOFS AESOPS Program in the western Pacific sector of the Southern Ocean:

Survey I, October 20–November 24, 1997; Process I, December 2, 1997–January 3, 1998; Survey II, January 8–February 8, 1998; and Process II, February 13–March 19, 1998. The primary goal of the "Survey" cruises was to conduct mesoscale surveys with towed SeaSoar instruments across the Polar Front. The "Process" cruises, on the other hand, spent more time at fixed stations conducting standard hydrographic casts and biogeochemical studies, and they covered a wider latitudinal range. For the Process cruises, most samples were collected during the "southbound" transect that ran along 170°W to the ice edge. The ice edge moved southward in response to seasonal warming, from $\approx$63°S during Survey I to south of $\approx$72°S during Process II. Limited sampling during the Process cruises also was conducted at selected stations during the "northbound" return transect. Successful ^{234}Th profiles were collected at 4 stations during Surveys I, 6 stations during II, and 10 stations each during Process cruises I and II (Fig. 1).

An introduction and overview of the AESOPS study are provided by Smith et al. (2000). The AESOPS cruises were designed to cross the major hydrographic and biogeochemical features in this sector of the Southern Ocean. Major changes in biogeochemical rates and stocks were observed during the progression from the austral spring to summer. Based upon these data and a prior study that divides the Antarctic Circumpolar Current into distinct frontal regions (e.g., Orsi et al., 1995), the following nomenclature defining the principal zonation is used: Central Subantarctic Zone (C-SAZ) 50–55°S; North of Antarctic Polar Front (N-APF) 55–59°S; Antarctic Polar Front (APF) 59–61.5°S; South of Antarctic Polar Front (S-APF) 61.5–65.5°S; South of Antarctic Circumpolar Current (S-ACC) 65.5–68°S; North of Ross Sea (N-RS) 68–72°S (Fig. 1).

2.2. Thorium-234 sampling and analyses

Samples for ^{234}Th, POC and bSi were collected with large-volume in-situ pumps. The procedures and analyses for ^{234}Th and POC are identical to those reported for the Ross Sea sampled one year earlier by our group (Cochran et al., 2000) and are only summarized here. Samples were typically obtained at depths of 5, 30, 55, 80, 105, 155 and 300 m. All samples were collected by hanging 7 battery-powered in-situ pumps at discrete depths, where 300–500 l of water were sampled during a 1–2 h pumping interval (flow rates = 4–8 l min^{-1}). Sample profiling for ^{234}Th was chosen over our prior vertically integrating approach (Buesseler et al., 1995, 1998) in order to provide depth-resolved estimates of export and remineralization, though the focus of this manuscript is on export from 100 m only.

Each sample was passed first through a pair of 142-mm diameter filters. The first filter consisted of a Teflon screen of 70 μm nominal mesh size. This was followed sequentially by a 1 μm nominal pore size quartz filter (QMA). A wide-mouth baffled opening on the pumps ensured that the particles were evenly distributed over the filter surface and eliminated wash off during retrieval of our samples. The filtered water passed through a pair of manganese oxide-impregnated filter cartridges (Hytrex II, 0.5 μm polypropylene; Hartman and Buesseler, 1994). Extraction efficiency, E, is calculated from the ratio of ^{234}Th activities on the first (MnA) and second (MnB) cartridges ($E = 1 - \mathrm{MnB}/\mathrm{MnA}$; Livingston and Cochran, 1987). In theory, some particles might pass though our 1 μm nominal pore size QMA filter and be caught on the 0.5 μm nominal pore size MnA cartridge, thus biasing the extraction efficiency. In practice, this fraction is either such a small percent of the ^{234}Th signal on the MnA cartridge, and/or our QMA filter may collect

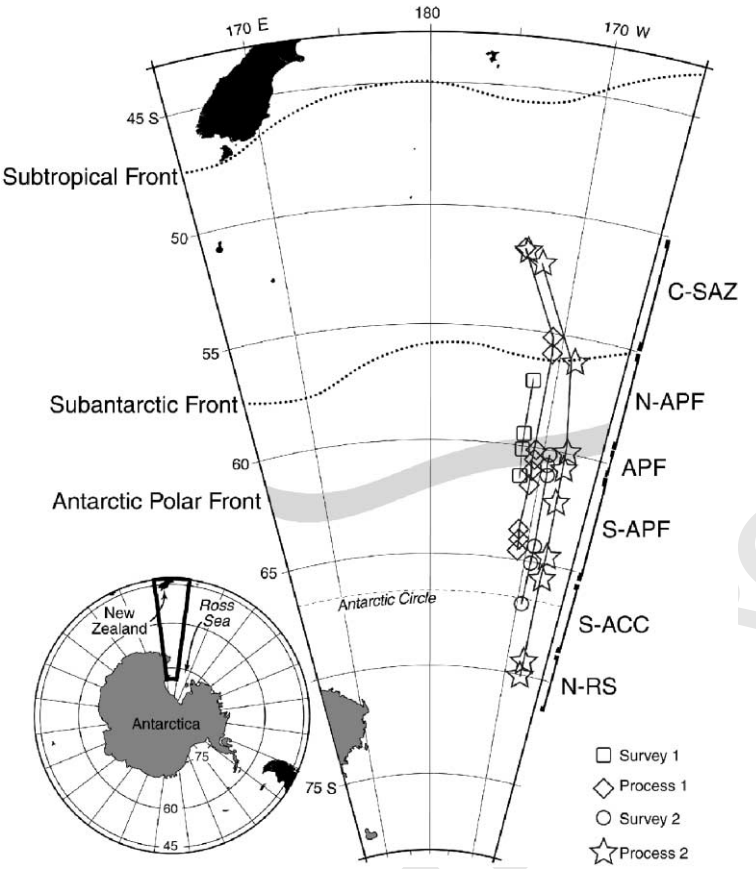

Fig. 1. Locations of sampling stations are shown for each of the four AESOPS cruises where ^{234}Th profiles were collected (the station position east/west of 170°W was adjusted slightly so that the station locations do not overlap on this diagram). Note that the southernmost station moved progressively south as the ice edge retreated during the sampling period (October 1997–March 1998). The approximate positions of the Subtropical Front, Subantarctic Front, and Antarctic Polar Front (APF) are also shown. In addition, the latitudinal bands where data were averaged are indicated: Central Subantarctic Zone (C-SAZ) 50–55°S; North of Antarctic Polar Front (N-APF) 55–59°S; Antarctic Polar Front (APF) 59–61.5°S; South of Antarctic Polar Front (S-APF) 61.5–65.5°S; South of Antarctic Circumpolar Current (S-ACC) 65.5–68°S; North of Ross Sea (N-RS) 68–72°S.

particles including those smaller than the nominal 1 μm pore size, such that we find complete agreement between this cartridge method and discreet dissolved and total ^{234}Th measurements (Buesseler et al., 2000a).

^{234}Th analyses were performed primarily at sea by direct gamma counting of the dried and crushed Mn cartridges (Buesseler et al., 1995, 1998) or direct beta counting of the filters (Buesseler et al., 1998; Cochran et al., 2000). The QMA filter was dried overnight after which 20 25 mm diameter subsamples were cut from the filter, stacked, pressed into a counting cup, covered with mylar and aluminum foil and beta counted. The Teflon screens were rinsed with prefiltered deep water immediately after collection to remove the particles, which were then deposited onto a

single 25 mm diameter 1.2 μm pore-sized Ag filter. The Ag filters were also dried, covered with mylar and foil, and beta counted directly for ^{234}Th. The Ag filters were later subsampled by weight in the shore laboratory for POC, PON and bSi analyses, while the QMA subsamples for CHN were taken from the original 142 mm filter. We have found no significant difference between replicate subsamples from the same filter. Presumably, particles are evenly distributed due to the design of our filter holder, which includes a wide baffled opening above, and wide support below the Teflon screen and QMA filter.

2.3. POC and bSi analyses

All CHN samples were treated via acid fuming to remove carbonate. We have complete profiles of POC for both 1–70 μm and > 70 μm particles with the exception of 1–70 μm POC for Survey II (due to accidental loss of the samples). Biogenic silica could not be determined on the QMA filters because of the large Si blank, but it was measured on a selected subset of the Ag filters. No bSi data are available from Survey II, as > 70 μm particles were rinsed onto QMA filters rather than Ag filters, and thus the bSi blanks were too high. The bSi samples were analyzed using the NaOH digestion procedure described by Brzezinski et al. (2000a). That procedure hydrolyzes the biogenic silica in hot NaOH and the resulting solution is analyzed for silicic acid concentration using the colorimetric method of Strickland and Parsons (1972) modified to use the reagent blank of Brzezinski and Nelson (1986). The original procedure was designed for polycarbonate filters and the application of the method to Ag filters results in a brown discoloration of the NaOH digests. The discoloration did not contribute to absorbance at 810 nm, where the absorbance of the reduced silicomolybdic acid species is measured. Standard additions of $Si(OH)_4$ to samples showed that the brown material did not interfere with the reaction chemistry. All samples were well within the detection limit of the method (0.5 nmol bSi per subsample). Parallel sets of bSi samples collected on 0.6 μm polycarbonate filters from bottle casts are available for many of these same AESOPS stations (Brzezinski et al., 2000a).

3. Results

3.1. Thorium-234

Total ^{234}Th activities are used here for the calculation of the export fluxes and the ratios of POC/^{234}Th and bSi/^{234}Th are needed to calculate POC and bSi export (see *POC and bSi fluxes derived from* ^{234}Th). Thus the inventory of total ^{234}Th in the upper 100 m and the ratio of particulate ^{234}Th to POC and bSi on the > 70 μm particles are the focus of this manuscript. The complete dissolved, 1–70 μm and > 70 μm ^{234}Th activity data are not shown here but can be found via the US JGOFS Data Management Office at the web site: http://usjgofs.whoi.edu/. All ^{234}Th activity data are decay corrected to the midpoint of sampling and errors are propagated from the one-sigma counting uncertainty. In addition, for dissolved ^{234}Th, the uncertainty on the cartridge extraction efficiency is also considered (average counting error for MnA = ±4–6%; average extraction efficiency error = ±2–3%).

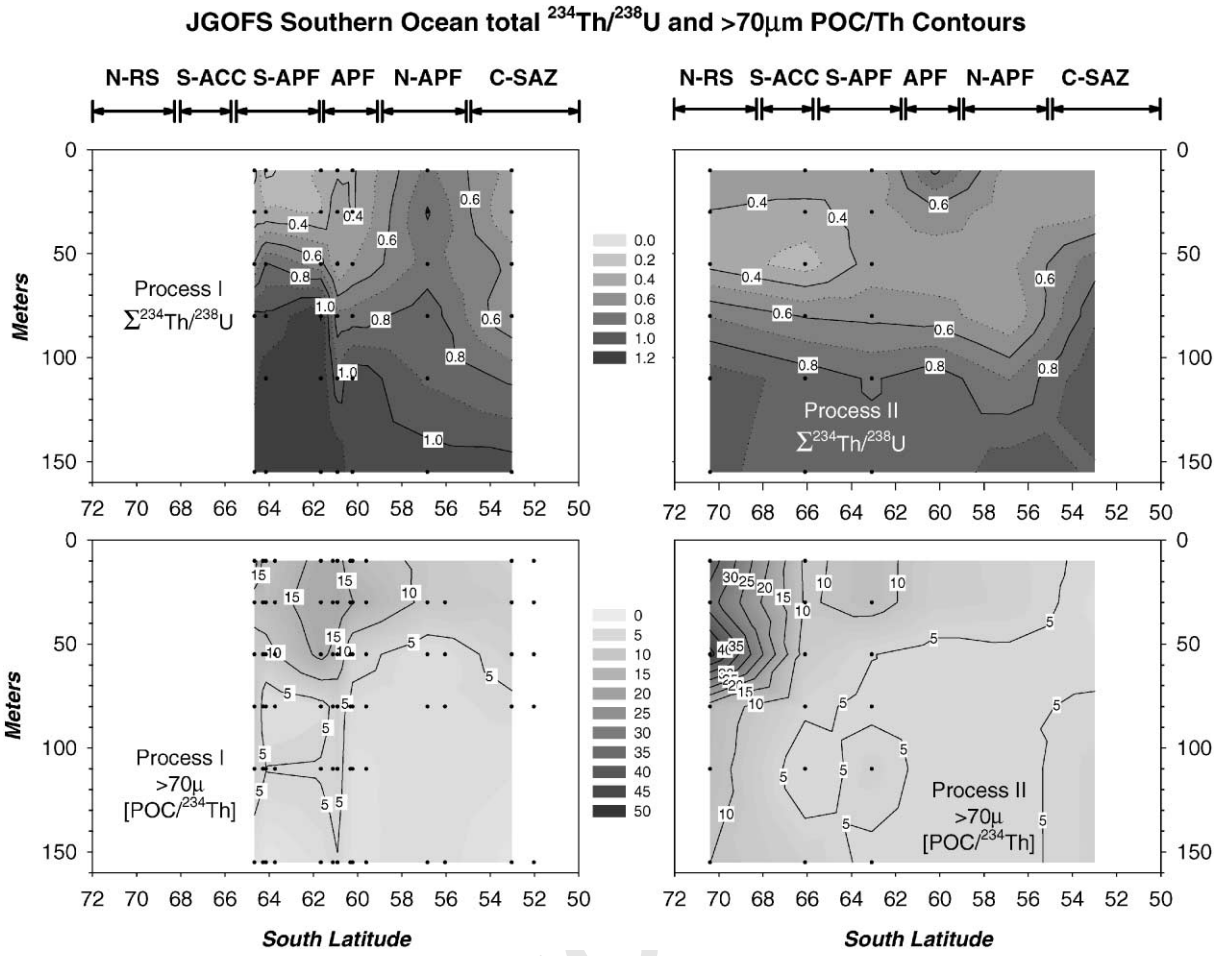

Fig. 2. Vertical sections of the total $^{234}Th/^{238}U$ ratio (upper panels) and > 70-μm POC/^{234}Th ratio (μmol dpm^{-1}; lower panels) vs. depth and latitude. Sampling depths are indicated by filled dots. The data shown were collected on the southbound leg of Process I (October 24–November 4, 1997) and on the southbound leg of Process II (January 17–28, 1998).

In general, particulate ^{234}Th in all size classes is highest in the surface waters, where total ^{234}Th activities are lowest. The particulate 1–70 μm ^{234}Th activities are 16% of the total ^{234}Th activity when averaged over all samples from depths less than 100 m, and 7% of the total between 100 and 300 m. Thorium-234 activities on the > 70 μm particles are small and variable, averaging only 14% of the 1–70 μm activities in samples from < 100 m to 7% in samples from > 100 m. Potential filtration artifacts associated with QMA and the Teflon screens are discussed in the following section on POC and bSi.

The pattern of total ^{234}Th is best seen in the data from the Process I and II southbound legs, where we have the most complete sampling coverage (Fig. 2, upper panels). During both Process I and II, $^{234}Th/^{238}U$ ratios were low in the euphotic zone and increased with depth. The low ratios

are due to biological particle production and export, which remove ^{234}Th from the surface layer. During Process I, there was a transition near the APF, with waters to the north being depleted in ^{234}Th to greater depth than to the south but with generally higher ^{234}Th/^{238}U ratios (0.5–0.9) in the upper 100 m. The ^{234}Th/^{238}U ratio dropped to <0.3 in the surface waters south of the APF during Process I, but the values <1 were confined to shallower depths, presumably because the mixed layer was shallower on average (<50 m;). By Process II, ^{234}Th/^{238}U ratios <1 were found at all depths, the lowest ^{234}Th/^{238}U values (<0.3–0.4) being associated with a subsurface minimum south of 65°S.

3.2. Particulate organic carbon and biogenic silica

As with particulate ^{234}Th, concentrations of POC were generally much higher on the 1–70 μm than on the >70 μm samples (>70 μm POC/1–70 μm POC = 4.5%, 17%, and 7% for Survey I, Process I and Process II in the upper 300 m). Throughout JGOFS and in other studies, POC concentrations obtained with 0.7 μm nominal pore size glass fiber filters (GF/F) or 1 μm QMA filters have been lower when large volume (>100–1000 l) in situ filtration was used rather than Niskin bottles (1–4 l) and shipboard filtration. One possible cause for this difference is a dissolved organic carbon blank, which would elevate the small volume, bottle-derived POC values, particularly in deeper waters (Moran et al., 1999). Since the volume filtered per unit area of filter is higher on the in-situ pump samples, artifacts related to sample loading cannot account for this difference, since the pump samples have higher loading, but lower POC concentration.

The blank/sorption process also has been found to affect particulate ^{234}Th data in our own studies (Buesseler et al., 1998; Benitez-Nelson et al., 2000). We found higher particulate ^{234}Th values associated with low flow rates or low volumes using GFF or QMA filters, which we attribute to a ^{234}Th sorption blank. It should also be remembered that we use the total ^{234}Th activities to calculate export fluxes, and biases in ^{234}Th partitioning onto large or small particles do not affect the total. We also do not use the 1–70 μm POC/^{234}Th or bSi/^{234}Th data in our flux calculations, since we regard the material caught on the 70 μm screen to be more representative of sinking material. There was a relatively small difference in the POC/Th ratio between the filter types (on average less than $\pm$30–40%), hence any operational biases in collecting POC and ^{234}Th particulates using QMA filters would not change our final flux patterns even if we were to use the QMA data (see Discussion).

Any filtration step is an operational procedure that might not collect all particle types of a given size without bias. For example, some particles may break up and pass through the 70 μm screen and would be included in the QMA fraction. Unlike the QMA samples, sorption blanks are not a significant problem for the 70 μm Teflon screens. Inefficient rinsing during transfer of the particles to the Ag filter might be an issue, so we analyzed rinsed 70 μm screens for ^{234}Th to estimate ^{234}Th retained on the screen. The rinsing efficiency averaged 65% for all of the cruises, and we corrected all of our >70 μm ^{234}Th, POC and bSi particulate data by this factor (mean = 65 $\pm$ 16%, $n=18$). Thus our absolute concentrations of ^{234}Th, POC and bSi in the >70 μm fraction suffer from some additional uncertainty due to this rinsing efficiency and our assumption of equal efficiency for ^{234}Th, POC and bSi. However, since we need only *total* ^{234}Th activities to calculate the ^{234}Th flux, any bias in our rinsing efficiency alters only the calculated ^{234}Th activity associated with the >70 μm fraction, which is on average only 1.5% of the total ^{234}Th activity. Since we attribute

higher sinking rates to the larger particles, we use the *ratio* of POC/^{234}Th on the $>70\,\mu m$ particles for the calculation of POC fluxes (or bSi/^{234}Th for the bSi fluxes). Thus, for estimating POC/^{234}Th, we do not need quantitative collection of $>70\,\mu m$ particles, only a representative sample. The $>70\,\mu m$ particles have been found through microscopic analysis to consist of intact large cells, cell fragments, fecal pellets and unidentified marine snow (Buesseler et al., 1998). Our in-situ pumps are not efficient at collecting live zooplankton on the screens.

The distribution of $>70\,\mu m$ POC/^{234}Th across the AESOPS transect can be seen in the Process I and II southbound legs (Fig. 2, lower panels). Generally, the ratio of POC/^{234}Th decreases between the surface and 100–150 m. Such a decrease has been seen in prior studies, and we attribute it to the preferential remineralization of POC relative to ^{234}Th on sinking particles (Buesseler et al., 1995, 1998; Bacon et al., 1996). The surface value of the POC/^{234}Th ratio increased towards the southernmost stations during both cruises. A single control on the POC/^{234}Th ratio (particle size, depth, or region) cannot be identified, but we have found an association between blooms of large diatoms and elevated POC/^{234}Th ratios (summarized in Buesseler, 1998). For the calculation of POC export from the ^{234}Th flux, an estimate of the POC/^{234}Th ratio of the sinking particles at the depth of interest (100 m in this study) is needed. The gradient in the $>70\,\mu m$ POC/^{234}Th ratio below the upper 50–80 m is very small, so we used the average from the 3 deepest samples (80–150 m) at each station for our flux calculations (see *POC and bSi fluxes derived from ^{234}Th*).

The mean C : N mole ratio on all cruises at all depths sampled for both the QMA filters and $>70\,\mu m$ screens was 5.7. With this ratio, one can convert from POC to PON flux. Due to the small sample sizes, especially in the $>70\,\mu m$ fractions, we have the possibility for significant PON analytical errors, hence we did not attempt to examine in detail the variability in C : N with depth, filter type or between cruises.

3.3. Calculation of thorium-234 fluxes

Thorium-234 activity is usually $<^{238}$U activity in the upper 100–200 m, the difference defining a deficit that tends to be largest in coastal settings and during blooms. The ^{234}Th balance in a given parcel of water is:

$$\partial^{234}\mathrm{Th}/\partial t = (^{238}\mathrm{U} - ^{234}\mathrm{Th})\lambda - P + V, \quad (1)$$

where ^{238}U is the uranium activity determined from salinity (^{238}U (dpm l^{-1}) = 0.07097 × salinity; (Chen et al., 1986), ^{234}Th is the measured activity of total ^{234}Th, λ is the decay constant for ^{234}Th ($=0.0288\,d^{-1}$), P is the net loss of ^{234}Th on sinking particles, and V is the sum of advective and diffusive effects on ^{234}Th. Solving for P and integrating to the depth of interest gives the export flux of ^{234}Th.

Usually, a 1-D steady-state (SS) process is assumed, in this case Eq. (1) simplifies to:

$$P = (^{238}\mathrm{U} - ^{234}\mathrm{Th})\lambda z\ 1000\,l\,m^{-3}, \quad (2)$$

where z is the depth of integration (here 100 m). Given that the ^{234}Th flux is driven by the difference between the ^{234}Th and ^{238}U activities, the propagated flux errors increase with depth (Coale and Bruland, 1987). The accuracy of any 1-D SS ^{234}Th-derived flux estimate depends upon the accuracy of the ^{234}Th measurements and the error introduced by ignoring advection and

diffusion and non-steady-state processes. A steady-state approach essentially assumes a constant flux over periods of days to weeks determined by the ^{234}Th decay time and residence time. Non-steady-state effects are important during periods of significant ^{234}Th drawdown, such as plankton blooms and the relaxation period following a bloom (Buesseler et al., 1992, 1998; Cochran et al., 1997), but not during other periods (Tanaka et al., 1983; Wei and Murray, 1991; Moran and Buesseler, 1993). The effect of upwelling has been found to be significant only in regions of high upwelling velocity, such as the equatorial Pacific (Buesseler et al., 1995; Bacon et al., 1996; Dunne and Murray, 1999) and coastal sites during the SW Monsoon in the Arabian Sea (Buesseler et al., 1998). Horizontal advection can be significant in nearshore sites, such as harbors, where intensified scavenging occurs around the margins (Portland Harbor; Gustafsson et al., 1998).

We calculated for each station, the 1-D SS flux of ^{234}Th both with and without an upwelling/downwelling term. Ekman pumping velocity at the base of the mixed layer was calculated from the mean climatological winds, and the velocities were averaged over monthly time intervals and 5 degree latitudinal bands (MacCready and Quay, personal communication). We deem the monthly averaging to be appropriate for ^{234}Th considering the half-life of ^{234}Th, and we have used monthly average velocities in previous studies (Buesseler et al., 1995, 1998). Since ^{234}Th increases with depth, higher upwelling rates yield higher particulate ^{234}Th flux to balance the additional supply from below.

The upwelling velocities were low, generally less than $0.1\,m\,d^{-1}$. Using these velocities and the measured vertical ^{234}Th gradient, we calculated for each profile the ^{234}Th flux associated with upwelling and found it always to be small, on average only 1.4% of the SS flux for Survey I, 4.2% for Process I, 3.1% for Survey II and 4.7% for Process II. We chose to neglect this term in the calculations reported here.

The ^{234}Th fluxes were calculated for each station and then averaged over common latitudinal bands for each of the four cruises (Table 1a). The fluxes were calculated at 100 m, which was consistently below the mixed layer and encompassed the 0.1% light level. The results ranged from 1800–3500 $dpm\,m^{-2}\,d^{-1}$, relatively high compared to other sites and seasons. For comparison, the highest fluxes associated with the SW Monsoon in the Arabian Sea were 5000 $dpm\,m^{-2}\,d^{-1}$ (annual mean $<2000\,dpm\,m^{-2}\,d^{-1}$; Buesseler et al., 1998). Peak fluxes in the 3000–3500 $dpm\,m^{-2}\,d^{-1}$ range were seen during the North Atlantic spring bloom (Buesseler et al., 1992); in the equatorial Pacific (Buesseler et al., 1995; Murray et al., 1996; Bacon et al., 1996) and north of the Weddell Sea (Rutgers van der Loeff et al., 1997), however, all had periods of considerably lower ^{234}Th flux not seen here. The fluxes along 170°W are much higher than those found in the northeast Pacific Ocean (200–1400 $dpm\,m^{-2}\,d^{-1}$; Charette et al., 1999) or at the Bermuda or Hawaii time-series sites (Buesseler et al., 2000b; Benitez-Nelson et al., 2000). Thus during the entire spring/summer period, despite the low productivities at these latitudes (Hiscock et al., 2000), there was efficient removal of ^{234}Th on sinking particles.

A further refinement can be obtained at selected latitudes where we have sufficient time-series data to apply a non-steady-state (NSS) model. For this calculation, we used the total ^{234}Th activities for a given latitudinal band to approximate $\partial^{234}Th/\partial t$ $(=(Th_2-Th_1)/(t_2-t_1)$, where Th_1 is the ^{234}Th activity at t_1, etc.; Buesseler et al., 1992). Given the limited sampling on the Survey cruises, this could only be done for six pairs of ^{234}Th activity data associated with the three time intervals between our four cruises (see NSS flux data, Table 1b). Generally speaking, if ^{234}Th activities are decreasing with time, the ^{234}Th flux P increases (NSS/SS flux >1). Conversely, if

^{234}Th activities are increasing, the NSS flux is lower (NSS/SS flux <1). When we compare the average of the SS flux calculated from t_1 and t_2, to the NSS flux between t_1 and t_2, we found differences that ranged from 11–40% in both positive and negative directions. Ideally, the NSS approach would be preferred, but the limited sampling opportunities did not allow for a full NSS

Table 1
Average fluxes and particle ratios

(a) Steady-state model[a]

Latitudinal bands	Survey I stations	^{234}Th flux dpm m^{-2} d^{-1} ±error	POC/^{234}Th[b] μmol dpm^{-1} ±error	POC flux mmol C m^{-2} d^{-1} ±error	Si/^{234}Th[b] μmol dpm^{-1} ±error	Si flux mmol Si m^{-2} d^{-1} ±error
October 24–November 4						
50–55°S[c]						
55–59°S[d]	1	2498±191	5.8±1.4	14.5±3.7	0.88±0.10	2.2±0.3
59–61.5°S[e]	8,12	2161±125	6.2±1.4	13.3±3.1	2.40±0.70	5.2±1.5
61.5–65.5°S[f]	3	2849±212	5.7±0.6	16.4±2.0	1.99±0.91	5.7±2.6
65.5–68°S[g]						
68–72°S[h]						
December 4–25						
	Process I stations					
50–55°S	1	3573±197	3.0±1.1	10.6±4.1	1.20±0.33	4.3±1.2
55–59°S	2,17	1796±184	3.1±0.9	5.5±1.7	0.86±0.10	1.5±0.2
59–61.5°S	4,5	3170±146	4.4±2.0	13.9±6.5	3.10±0.40	9.8±1.3
61.5–65.5°S	6,7,8,9	2440±93	4.5±1.6	11.0±3.9	2.55±0.40	6.2±1.0
65.5–68°S						
68–72°S						
January 13–28						
	Survey II stations					
50–55°S						
55–59°S						
59–61.5°S						
61.5–65.5°S	4,5,6,8	3480±778	6.6±2.0	22.9±8.7	No Si	
65.5–68°S	3	3066±145	5.2±0.6	16.0±2.0		
68–72°S						
February 16–March 15						
	Process II stations					
50–55°S	1,29	2445±250	3.8±0.7	9.3±1.9	0.59±0.15	1.4±0.4
55–59°S	2	3746±109	4.3±0.3	16.0±1.1	1.89±0.22	7.1±0.8
59–61.5°S	4	2755±78	4.3±0.4	11.8±1.2	3.08±1.17	8.5±3.2
61.5–65.5°S	7,18,20	2467±1040	4.7±1.3	11.6±5.9	4.47±0.35	11.0±4.7
65.5–68°S	9	3788±152	5.1±1.7	19.4±6.5	1.70±0.50	6.4±1.9
68–72°S	13,15	3134±333	14.2±5.2	44.4±17.0	1.71±0.35	5.4±1.2

Table 1 (*continued*)

(b) Non-steady state model[i]

Latitudinal bands	^{234}Th flux dpm m^{-2} d^{-1} ±error	POC/^{234}Th[j] μmol dpm^{-1} ±error	POC flux mmol C m^{-2} d^{-1} ±error	Si/^{234}Th[j] μmol dpm^{-1} ±error	Si flux mmol Si m^{-2} d^{-1} ±error
October 30–December 15					
50–55°S[c]					
55–59°S[d]	1680 ± 458	4.4 ± 1.4	7.5 ± 3.1	0.87 ± 0.01	1.5 ± 0.4
59–61.5°S[e]	3602 ± 336	5.3 ± 0.9	19.0 ± 3.7	2.75 ± 0.35	9.9 ± 1.6
61.5–65.5°S[f]	2360 ± 265	5.1 ± 0.6	12.1 ± 2.0	2.27 ± 0.28	5.4 ± 0.9
65.5–68°S[g]					
68–72°S[h]					
December 15–January 20					
50–55°S					
55–59°S					
59–61.5°S					
61.5–65.5°S	3950±1072	5.5±1.0	21.9±7.2	2.55±0.40	10.1±3.2
65.5–68°S					
68–72°S					
January 20–March 1					
50–55°S					
55–59°S					
59–61.5°S					
61.5–65.5°S	2122±1512	5.6±0.9	12.0±8.7	4.47±0.35	9.5±6.8
65.5–68°S	4032±239	5.2±0.0	20.8±1.2	1.70±0.50	6.9±2.1
68–72°S					

[a] 1D steady state fluxes at 100 m are averaged for the appropriate latitudinal bands for each of the four AESOPS cruises.

[b] POC/^{234}Th and Si/^{234}Th ratios are averaged over 80–150 m for > 70 μm particles. The error represents the deviation between samples, or the minimum ^{234}Th counting error, whichever is larger.

[c] Central Subantarctic Zone.

[d] North of Antarctic Polar Front.

[e] Antarctic Polar Front.

[f] South of Antarctic Polar Font.

[g] South of Antarctic Circumpolar Current.

[h] North of Ross Sea.

[i] 1D Non-steady state model is used to calculate 100 m fluxes during the 3 time intervals between the AESOPS cruises. This can only be done for 6 latitudinal bands (see text for discussion). Fluxes are calculated from the midpoint of Survey I to the midpoint of Process I, etc.

[j] POC/^{234}Th and Si/^{234}Th ratios are the averages from 80–150 m for > 70 μm particles collected on the paired cruises used for the NSS model, except for January 20–March 1 Si/^{234}Th ratios, when Process cruise II bSi data only are available.

treatment of these AESOPS cruises. We therefore only use this comparison of the NSS and SS model as one estimate of the overall uncertainty of our methods. For further discussion in this paper, we use the SS model in general, but we also report the NSS fluxes for POC and bSi when sufficient data are available (Table 1a = SS; Table 1b = NSS fluxes).

3.4. POC and bSi fluxes derived from ^{234}Th

The calculation of POC (or bSi) flux is straightforward:

$$\text{Flux} = (E/^{234}\text{Th})P, \tag{3}$$

where P is the ^{234}Th flux as discussed above (dpm m^{-2} d^{-1}), and $E/^{234}$Th is the measured ratio of an elemental constituent (POC, bSi, PON, etc.) and particulate ^{234}Th on sinking particles. As summarized in Buesseler (1998), this empirical approach hinges on two assumptions. First, the export flux of ^{234}Th must be accurately estimated from the ^{234}Th activity balance (Eq. (1)). Secondly, the particles that are analyzed for ^{234}Th and elemental composition must be characteristic of those carrying the element of interest below the euphotic zone. We use the variability in the POC/^{234}Th ratio on the QMA vs. Teflon screens, i.e., small vs. large particles, to place constraints on this ratio. In the equatorial Pacific, both size-fractionated filtration and shallow traps were used to determine the POC/^{234}Th ratio, and the ratio was approximately 2 times higher in the traps (Murray et al., 1996). There were no shallow traps deployed during AESOPS for comparison here. We prefer to use in-situ filtration in any case since we have shown that trap biases can sort POC and ^{234}Th bearing particles (Buesseler et al., 2000a). The POC and bSi flux results for the individual stations, based on the SS model, are shown in Fig. 3 for the discrete stations, and are provided as averages across latitudinal bands for both SS and NSS models in Table 1. The error in Table 1 on C/Th and bSi/Th includes both the analytical error in determining bSi, POC and ^{234}Th, and the variability in the data points that are averaged.

POC fluxes ranged from 11–16 mmol C m^{-2} d^{-1} during late October/early November and dropped slightly during December to values in the 5–10 range, though there is considerable overlap with the earlier time period. The biggest increase in POC flux can be seen in the early part of 1998 and during the austral summer. The later fluxes are as high as 50 mmol C m^{-2} d^{-1}, with the highest values at the southernmost stations in the Ross Sea Gyre water at 69–72°S. The highest fluxes were thus in recently open waters that had been ice covered. By the end of the Process II cruise, the POC fluxes had dropped at the Polar Front and the more northern stations as the bloom progressed southward (Fig. 2b; open diamonds; March 6–15). The NSS fluxes for POC are on the order of 10–20 mmol C m^{-2} d^{-1}, overlapping with the SS fluxes, though the temporal and spatial coverage is limited to the regions closer to the Polar Front (Table 1b). Relative to other studies, it should be noted that these export fluxes are large, especially when compared to local chlorophyll or primary productivity rates (see Discussion).

Biogenic silica fluxes show a somewhat different pattern in space and time than those for POC. bSi fluxes ranged from <1 to almost 15 mmol Si m^{-2} d^{-1} for the individual stations, and from 1.5 to 10 when the latitudinal averages and the NSS model were used (Table 1a and b). Similar to the POC fluxes, the bSi fluxes were highest in the summer (no bSi data are available for Survey II), but they peaked further north in the latitudinal band between the APF and the Southern Antarctic Circumpolar Current Front (SACCF) (61.5–65.5°S) where there was a seasonal drawdown of silicic acid from >40 to <5 μmol and occasionally <1 μmol in surface waters (Brzezinski et al., 2000a). There has been only one prior attempt to use ^{234}Th to derive bSi fluxes, and this was for the German JGOFS cruises in the Weddell Sea region (Rutgers van der Loeff et al., 2000). They reported non-bloom fluxes of 2–3 mmol Si m^{-2} d^{-1} for these same depths near

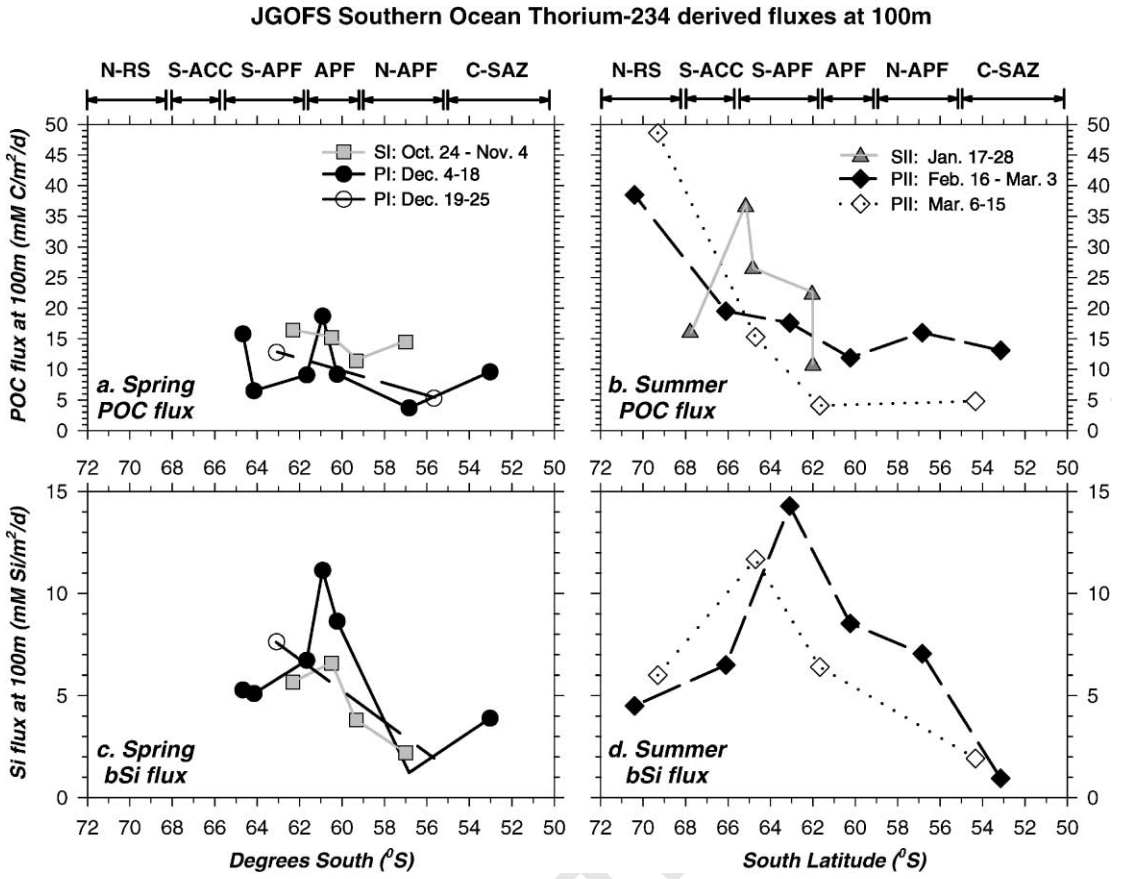

Fig. 3. Fluxes of POC (μmol C m^{-2} d^{-1}) and bSi (μmol Si m^{-2} d^{-1}) at 100 m vs. latitude derived from ^{234}Th data and a 1-D SS model. Panels a and c show the flux data for the austral spring cruises broken down into three sets of curves representing Survey I and Process I south and northbound legs, while panels b and d show the same fluxes for the summer cruises represented by Survey II and Process II south and northbound legs.

the Polar Front, and up to 12–25 mmol Si m^{-2} d^{-1} during bloom conditions, though their Si fluxes during the bloom were derived for somewhat greater depths (200 m).

4. Discussion

A major finding of this study is the relatively high ^{234}Th deficiencies and hence the elevated fluxes of POC and bSi fluxes during the spring/summer growth cycle across the Polar Frontal region. There are also strong seasonal changes in these fluxes with latitude and a difference in the spatial patterns of POC and bSi export (Fig. 3). Moore et al. (1999) used SeaWiFS ocean-color images to define the mean surface chlorophyll patterns specific to the four AESOPS cruises. During Survey I, chlorophyll levels were relatively low north of the APF, but there was already a small bloom underway near the APF, with mean chlorophyll concentrations around 0.3 mg m^{-3}.

The mixed layers shoaled from 150 m to 60–80 m during this period, and the sea ice extended to just south of 62°S. Primary production rates near the APF ranged from 20–50 mmol C m^{-2} d^{-1} (Hiscock et al., 2000), and silica production rates ranged from 7–17 mmol Si m^{-2} d^{-1} (Brzezinski et al., 2000a). Export derived from ^{234}Th was on the order of 10–15 mmol C m^{-2} d^{-1} and 6–11 mmol Si m^{-2} d^{-1}.

By the time of Process I, mixed layers were as shallow as 30 m and the sea ice retreated from 63°S to 66°S during the cruise. Average chlorophyll concentrations had increased to a mean of 0.5 mg m^{-3} along 170°W, with enhanced levels in the northern stations in the central Subantarctic Front zone. An intense bloom of diatoms with [bSi10 μmol Si l^{-1} was observed associated with the retreating ice edge south of the APF near the ice-edge at ca. 63°S (Brzezinski et al., 2000a). Primary production followed the same pattern with highest rates in the C-SAF and near the ice edge (100–150 mmol C m^{-2} d^{-1}; Hiscock et al., 2000). Silica production rates increased from those observed during Survey I to values between 20 and 37 mmol Si m^{-2} d^{-1} within the diatom bloom (Brzezinski et al., 2000a). The latitudinal pattern of POC export flux was relatively uniform at this time, ranging from 10–14 mmol C m^{-2} d^{-1}. The flux of bSi was highest (6.2–9.8 mmol Si m^{-2} d^{-1}) in the diatom bloom between the APF and SACCF and was 4–6 times lower (1.5 mmol Si m^{-2} d^{-1}) north of the APF (Table 1a).

By the time of the second survey cruise, Moore et al. (1999) saw a decline in the regional mean surface chlorophyll levels to 0.3 mg m^{-3}, with the highest values (>1 mg m^{-3}) clearly associated with the Ross Sea gyre water to the south of 70°S. There were no primary productivity studies on this cruise, but siliceous biomass reached its seasonal maximum at this time with bSi concentrations of 10–16 μmol Si l^{-1} within the diatom bloom (Brzezinski et al., 2000a). The diatom bloom had progressed southward to ca. 65°S, leaving a zone of low siliceous biomass and low surface silicic acid concentrations in its wake (Brzezinski et al., 2000a). POC export increased by 50% compared to the previous cruise, to 16–22 mmol C m^{-2} d^{-1} in the region just south of the APF where the diatom bloom had been located roughly one month earlier.

By Process II, mean regional chlorophyll levels had dropped to <0.2 mg m^{-3} along 170°W. There was no evidence of a diatom bloom anywhere in the region (Brzezinski et al., 2000a). Both total primary productivity and silica production rates had declined to relatively low rates across the entire AESOPS line south of 55°S (mean = 20 mmol C m^{-2} d^{-1}, Hiscock et al., 2000, and 5.5 mmol Si m^{-2} d^{-1}, Brzezinski et al., 2000a). During this final cruise, we saw the highest export fluxes of POC at the stations in the Ross Sea gyre water near 70°S (40–50 mmol C m^{-2} d^{-1}) and they were still high north and south of the APF (15 mmol C m^{-2} d^{-1}) on the northbound leg, dropping to lower levels during the last two stations in early March at the APF and at 54°S (5 mmol C m^{-2} d^{-1}). Biogenic silica fluxes increased by nearly 200% from those observed during Process I reaching 11.0 mmol Si m^{-2} d^{-1} in the latitudinal zone previously occupied by the diatom bloom (61.5–65.5°S, Table 1a). As shown in Fig. 2, the magnitude of the flux ranged from 5–15 mmol Si m^{-2} d^{-1} between the APF and SACCF, which is on the same order as Si uptake rates measured at the same time and stations (Brzezinski et al., 2000a).

The relationship between production and export was not fixed. Primary and silica production followed the southward progression of the diatom bloom as the ice edge retreated, and were accompanied by the drawdown of nutrients and dissolved inorganic C and Si stocks between the APF and SACCF (Brzezinski et al., 2000a; Sigmon et al., 2000). Export of POC and bSi lag the productivity maxima by 1–2 months, although the duration of the lag is uncertain due to the lack

of primary productivity and bSi export data during Survey II. Also, it must be considered that tracer incubations for primary productivity and silica production are conducted for only 12–24 h periods, whereas ^{234}Th averages over periods of days to weeks determined by its decay time and residence time. Thus low ^{234}Th upon arrival at a given station represents high export *prior* to the occupation. In other studies we have seen significant delays between the onset of production and the export of POC, for example in the North Atlantic Bloom Experiment (Buesseler et al., 1992), Arabian Sea (Buesseler et al., 1998), Ross Sea (Cochran et al., 2000) and during a study of the response of the marine ecosystem to Fe fertilization (Bidigare et al., 1999). The same pattern of a delay in shallow export response seen with ^{234}Th also was found in the AESOPS 1000 m sediment trap record (Honjo et al., 2000), where trap fluxes peak at roughly the same time as the ^{234}Th fluxes during the January through March time period.

These delays between production and export result in extremely high export ratios, implying the very efficient removal of POC via sinking particles relative to C uptake during the period following high production events (ThE > 30–50% = ^{234}Th derived export flux/^{14}C derived primary productivity; Buesseler, 1998). Seasonal averaged primary production rates at the APF were 34 mmol C m^{-2} d^{-1}, and POC export was roughly half of this value (18 mmol C m^{-2} d^{-1}, ThE = 54%). The export ratio is commonly < 10% in other open ocean settings, but higher values are associated with seasonal diatom blooms (Buesseler, 1998). In contrast perhaps to other sites where production and export are both elevated during blooms, the community structure in the Southern Ocean leads to relatively high export ratios even during the lowest productivity periods.

The ThE ratio for bSi also shows a dramatic increase between Process I and Process II. Brzezinski et al. (2000a) report average silica production rates in the 60–66°S latitudinal band of 27.4 and 5.5 mmol Si m^{-2} d^{-1}, for Process I and II, respectively. Combined with the bSi fluxes in Table 1a these rates imply ThE ratios of 0.27 and 1.89 for bSi during Process I and II, respectively. The lower rate observed during the active bloom sampled during Process I suggests that 73% of the silica production at that time was retained in the surface water. By the time of Process II, export exceeded production by almost 200%. ThE ratios > 1 cannot be sustained. We believe that the very large export ratio for bSi observed during Process II is a consequence of the different time scales measured by the Th-flux method that integrates over approximately a month time scale versus surface water silica production rates determined using 24 h bottle incubations (Brzezinski et al., 2000a). The high ThE ratio for bSi is consistent with the collapse of the diatom bloom between Survey II and Process II that removed over two-thirds of the bSi from the upper water column (Brzezinski et al., 2000a). The time scale represented by the Th-based flux method would encompass the large flux of biomass associated with the demise of the bloom between cruises, while the low silica production rates observed during Process II represent rates of silica production occurring after that large export event. The large loss of bSi from surface waters is still recorded by the ThE ratio despite the difference in time scales represented by the Th methods and short-term bottle experiments.

4.1. Prior ^{234}Th based estimates of particulate export in the Southern Ocean

Shimmield and Ritchie (1995) measured ^{234}Th at a single station near the ice front during December 1992 in the Bellingshausen Sea (67° 37′S; 84° 58′W). Using their ^{234}Th data and a POC/^{234}Th measured at 100 m on filters (= 6.5 μmol dpm^{-1}), one obtains a POC flux of

10 mmol C m^{-2} d^{-1}, similar to our December 1997 fluxes from our southernmost stations near the ice-edge (13–15 mmol C m^{-2} d^{-1} at 63.0°S and 64.7°S), though not as high as the late summer fluxes we observed further south in the Ross Sea Gyre water (up to 80 mmol C m^{-2} d^{-1}; Cochran et al., 2000). Rutgers van der Loeff et al. (1997, 2000) sampled extensively for ^{234}Th along the German JGOFS line near 6°W during both the austral spring (October–November 1992) and summer (December 1995–January 1996). The spring data were strongly time-dependent, and a non-steady-state ^{234}Th model was needed to account for the shift to lower ^{234}Th activities, particularly in the region at and just north of the Polar Front (near 50°S in the Weddell Sea). Their peak POC fluxes were 20–40 mmol C m^{-2} d^{-1} in the vicinity of the Polar Front (C/Th ratio of 6–12 μmol dpm^{-1}) with a sharp drop to the south where chlorophyll levels were lower. During their summer cruises, Rutgers van der Loeff found nearly constant ^{234}Th activities and a lower POC flux of around 10 mmol C m^{-2} d^{-1} between the Polar Front and the receding ice edge. They argue that this lower flux might be typical of much longer periods of the year relative to the shorter spring bloom conditions sampled in 1992, so that the lower summer fluxes might account for a higher percentage of annual export.

The studies by Rutgers van der Loeff et al. (1997, 2000) and by us show large seasonal and latitudinal variability in export in the Southern Ocean. This makes direct comparison of different data sets difficult. Our peak POC fluxes at the Polar Front are 10–15 mmol m^{-2} d^{-1} with a 1-D SS model, or up to 19 mmol C m^{-2} d^{-1} if we use the NSS model between Survey I and Process II (Table 1). Thus to a first order, these fluxes are similar. Unlike those of Rutgers van der Loeff et al. (2000), our highest POC fluxes were found farthest south in the late summer, but this southernmost bloom appears to be in a region more characteristic of the Ross Sea than the Polar Frontal Zone. Biogenic silica fluxes by Rutgers van der Loeff et al. (2000) for the Polar Frontal Zone near 6°W range from 13–26 mmol Si m^{-2} d^{-1} during the late November bloom to 2–3 mmol Si m^{-2} d^{-1} later in the austral summer. Our study shows less of a seasonal change in the flux of bSi, although the pattern observed was the opposite of that reported by Rutgers van der Loeff et al. (2000), with lower fluxes in the November/December time frame and bSi flux increasing later in the year. They also found higher rates earlier in the season and the POC and bSi flux peaks were more tightly coupled in their study area. Such difference cannot be explained with the currently limited data sets, but they are not inconsistent with the known high variability of seasonal production in the Southern Ocean.

During January–April 1997, we found POC export in the Ross Sea to range from essentially zero early in the austral spring and late summer, to as high as 40–80 mmol C m^{-2} d^{-1} in January–February (Cochran et al., 2000). The peak fluxes in the Ross Sea are some of the highest export fluxes obtained anywhere with the ^{234}Th method. Thus POC fluxes of 40–50 mmol C m^{-2} d^{-1} in the region just north of the Ross Sea sampled during Process II, appear to be more similar in magnitude to the blooms in the Ross Sea proper than near the Polar Front (Cochran et al., 2000). A study in the Ross Sea by Langone et al. (1997) did not estimate POC flux directly, but from their ^{234}Th data (two depths only in upper 100 m at three stations) and our own C/Th ratios, POC export would range from zero to 5–10 mmol C m^{-2} d^{-1} (December 1994), similar to the Cochran et al.'s (2000) low export estimates during early spring in the Ross Sea.

There are no other ^{234}Th data in the Antarctic, but there have been a few studies at high latitudes in the Northern Hemisphere. Fluxes as high as 38 mmol C m^{-2} d^{-1} in the Chukchi Sea (Moran and Smith, 2000) and 35 mmol C m^{-2} d^{-1} in a Greenland Polynya (Cochran et al., 1995)

have been found using the ^{234}Th method. Under the Arctic ice (and presumably under the Antarctic ice), export fluxes are significantly lower, ranging from <1 to $7\,\mathrm{mmol\,C\,m^{-2}\,d^{-1}}$ (Moran and Smith, 2000). In the Arctic, some of the apparent ^{234}Th removal under the ice may be driven by process at the margins and horizontal transport of ^{234}Th-depleted waters into the basin interior. As we approach the land/ice edge in Antarctica, we will also need to consider margin removal as a control on the local vertical ^{234}Th distribution. Evidence of $^{234}\mathrm{Th}/^{238}\mathrm{U} < 1$ below 100–200 m has been taken as an indication that such processes are taking place. This has been seen in selected ^{234}Th profiles near the Antarctic continent in the studies by Shimmield and Ritchie (1995) and Rutgers van der Loeff et al. (1997), but it would not be an issue in the Polar Frontal region.

It is worth noting that POC export was high relative to primary production during all cruises, from the onset of the first survey cruise to the late summer, when productivity had decreased. Rutgers van der Loeff et al. (2000) also noted that from the subantarctic frontal zone to the ice edge, ^{234}Th and hence POC fluxes were low but significant (POC flux avg. = $8–12\,\mathrm{mmol\,C\,m^{-2}\,d^{-1}}$), even during the summer months, when productivity and chlorophyll levels had declined. In another sector of the Southern Ocean south of the APF (61°S 140°W), we measured a "post-bloom" ^{234}Th deficit in a region of low chlorophyll at the start of an Fe enrichment study in early February 1999 (Charette and Buesseler, 2000). Thus all of these studies point to a high efficiency for particle export that is decoupled from the changes in surface chlorophyll or primary production maxima earlier in the season. Since grazing rates in these waters are generally low, one might attribute this post-bloom flux to the sinking of intact diatoms in response to some limitation in growth (major nutrient or Fe) or mixing. The exact cause of the diatom "crash" is not well understood, but the generally deeper mixed layers and higher surface nutrient concentrations observed during Process II compared to those measured less than two weeks earlier during Survey II imply that the bloom may have ended with the onset of increased vertical mixing.

4.2. Relative export flux of bSi and POC vs. depth

Biogenic silica export reached a pronounced maximum near 63–65°S during summer while POC export was relatively flat over the same meridional zone peaking further to the south (Fig. 3). This leads to a separation in the bSi and POC flux maximum that is quite striking in these data. When the ratio of bSi/POC flux is plotted vs. latitude there is a clear Si/POC peak centered south of the Polar Front on all cruises (Fig. 4). The absolute magnitude of this peak increases throughout the season, ranging from a Si/POC molar ratio of 0.4 to >1 by the end of the AESOPS cruises. These ratios are quite elevated compared to the value typically observed for nutrient-replete diatoms (Brzezinski, 1985). Measured gross Si : C uptake ratios in the surface waters averaged 0.15 during Process I and 0.04 during Process II (Brzezinski et al., 2000b). Those ratios are clearly less than the Si/C export ratio, indicating the preferential recycling of POC relative to bSi in surface waters and thus the operation of an efficient silicate pump (Dugdale et al., 1995). The largest relative drawdown in Si stocks in the water column also takes place in the region between the APF and the SACCF of the Polar Front (Brzezinski et al., 2000), and microscopic analyses indicates a predominance of large centric diatoms in the region of the Polar Front (Brown and Landry, 2000).

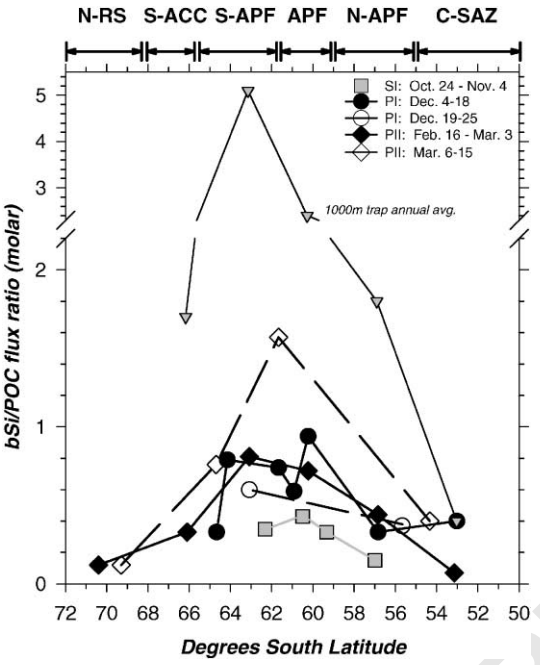

Fig. 4. Flux ratios of bSi/POC at 100 m are plotted vs. latitude for the AESOPS cruises and compared to the same ratio in the 1000 m sediment trap. The bSi/POC flux ratio at 100 m is taken from the data plotted in Fig. 3, and these data are plotted as curves associated with each cruise or leg as organized in Fig. 3. The 1000 m data are taken from the annual average provided by Honjo et al. (2000). Note break in axis in vertical scale which shows the molar ratio of bSi/POC.

What is also interesting in the Si : C flux comparison is that the same meridional pattern derived from ^{234}Th at 100 m also shows up in the moored sediment trap record from 1000 m presented by Honjo et al. (2000) from the same AESOPS transect (Fig. 4). Based on bottom-tethered time-series traps from November 1996 through December 1997, Honjo et al. (2000) concluded that the flux of biogenic material at 1000 m for the Polar Front region is about twice the estimated ocean wide average for POC, with a peak in bSi flux just south of the Polar Front. They calculated an annual average 1000 m bSi/POC flux ratio ranging from 0.4 at the northernmost mooring (53°S; only 2000 m data available) to 5.1 at 63°S, dropping significantly on either side of this maximum (Fig. 4). This same latitudinal pattern in the annual trap flux ratios would hold only if the trap data collected from October 1996 to December 1997 are used, which is the time period of direct overlap with our ^{234}Th data.

Comparison of Th based export at 100 m to sediment traps at 1000 m and below shows that the preferential recycling of POC over bSi observed in the surface waters continues as particles sink through deeper waters. Given the sampling time period for the traps (ending in December, 1997) and the lack of bSi fluxes in our study during Survey II, we can only compare directly the absolute magnitude of the fluxes during the Survey I and Process I time periods (late October to end of December, 1997). During this time period, only 1–3% of the POC flux leaving 100 m reaches the 1000 m trap (Table 2). This contrasts with bSi, for which 7–11% of the 100 m bSi flux is found in the 1000 m trap. Thus for bSi, this export efficiency is quite high, leading to the increase in bSi/POC ratios in the deeper samples. Two recent studies suggest that moored conical traps $\leqslant$1000 m

Table 2
Summary of 100 and 1000 m POC and bSi fluxes: October–December, 1997

Latitude band		100 m[a]	1000 m[b]	1000 m/100 m
APF	POC[c]	13.6	0.4	3%
59–61.5°S	Bsi[d]	7.5	0.84	11%
S-APF	POC[c]	13.7	0.10	0.7%
61.5–65.5°S	bSi[d]	6.0	0.42	7%

[a] ^{234}Th derived, 1-D SS model, from Process I and Survey 1: October 24–December 25, 1997, this manuscript.
[b] 1000 m trap data from Honjo et al. (2000) mooring 3 at 60°S and mooring 4 at 63°S, corresponding to APF and S-APF, respectively. Flux from trap cups collecting October 17–December 23, 1997 only.
[c] Average POC flux in mmol POC $m^{-2} d^{-1}$.
[d] Average bSi flux in mmol Si $m^{-2} d^{-1}$.

generally under collect the true net flux by 30–50% (Yu et al., 2000; Scholten et al., 2000). If this holds, then the 1000 m trap flux data would be too low and these 1000/100 m flux ratios would be even higher. The data at hand do not allow us to address this issue further. In any case, the export efficiency of bSi is quite high, and always much greater than that for POC.

The high export fluxes of bSi at both 100 and 1000 m together provide some of the strongest evidence to date to answer the long-standing puzzle of whether enhanced fluxes or preservation are responsible for the high accumulation of biogenic opal and carbon in the sediments below the APF (Nelson et al., 1995; DeMaster et al., 1996; Queguiner et al., 1997; Pondaven et al., 2000). Taken together, these ^{234}Th and trap results suggest that the high sedimentary opal accumulation found south of the APF is due to high bSi export. Furthermore, these high bSi/POC ratios in the 100 m data are consistent with the localized growth of diatoms that are characterized by thicker frustules. Recent studies suggest that low Fe conditions result in diatoms with thicker frustules that sink faster (Hutchins and Bruland, 1998) and the trend of higher bSi/POC in the 100 m export flux as one moves further south would follow this trend. Preliminary AESOPS Fe data suggest that the lowest surface Fe concentrations are found in the south, with extremely low values during Process II from the Polar Front southwards (Measures and Vink, 2000) and net Si : C and Si : N production ratios are all significantly elevated relative to Redfield (Brzezinski et al., 2000b). The reason for the sharp drop-off in bSi/POC ratio further south in our data and in the deep traps may be due to an ecological shift to different classes of diatoms with lower Fe requirements and lower Si : C ratios. There does appear in these AESOPS data a shift from the large centric diatoms associated with the APF to smaller pennate forms at the southernmost stations during Process II (Brown and Landry, 2000). These communities in the late summer found near 70°S appear more closely related to the Ross Sea blooms, which have very high POC export and lower relative Si fluxes.

5. Summary

These new data and other flux studies using ^{234}Th suggest that POC and bSi export in the Southern Ocean can reach some of the highest levels globally. This is despite relatively short

growth cycles and low productivity rates. Thus one general conclusion is that the Southern Ocean is characterized by one of the ocean's most efficient biological pumps. It is likely that the efficiency of export is related to the relatively high abundance of diatoms and low grazing rates associated with these waters. Within the general pattern of high export, we see a seasonal progression of increased POC and bSi export late in the austral spring/summer cycle. Thus while chlorophyll and primary productivity levels are highest in the austral spring, export lags production by one to two months.

For POC, the highest export rates are found farthest south (up to 50 mmol C m^{-2} d^{-1}), specifically in the Ross Sea Gyre water near 70°S in late February and early March. Biogenic silica fluxes on the other hand, peak during the same cruise, but the highest fluxes are found between the APF and the SACCF (up to 15 mmol Si m^{-2} d^{-1}). We attribute this separation in the POC and bSi flux peaks to the predominance of large centric diatoms in the region of the APF which may have higher Si : C ratios. This same pattern of highest Si : C just south of the APF is also found in the 1000 m trap data of Honjo et al. (2000). Taken together, these two export records suggest that the high accumulation rates of bSi in the sediments near the APF are a result of higher export rates, and minimal remineralization of bSi during sinking. As one moves further south of the ACC and into the Ross Sea, the flux appears to be dominated by smaller pennate diatom species, with a lower Si : C ratio. During the relatively short ice-free period at these southernmost stations, the POC fluxes reach some of the highest levels found in the upper ocean. While the temporal and spatial variabilities in export in this region are large, in all cases the relative rates of export on sinking particles are high here relative to most other regions. The combination of high nutrients, low grazing pressure and efficient transport of POC and bSi to depth on sinking particles appears to be responsible for this highly efficient biological pump in the region of the Polar Front and southward in the seasonal ice zone of the Southern Ocean.

Acknowledgements

We acknowledge the help of the officers and crew of the *R/V Revelle* and the four chief scientists: T. Cowles, R. Barber, K. Coale and W. Gardner. In addition, G. Crossin, H. Feng and P. Landry were of great help to our field program. We also acknowledge P. MacCready and P. Quay for providing the physical upwelling rates used in our ^{234}Th models and Janice Jones for technical assistance in developing the procedures to measure [bSi] on Ag filters. This work was supported primarily by US National Science Foundation grants to Buesseler, Bacon, Brzezinski and Cochran as part of the US JGOFS Program. This is WHOI contribution # 10328, SUNY contribution #1206 and US JGOFS contribution #566.

References

Bacon, M.P., Cochran, J.K., Hirschberg, D., Hammar, T.R., Fleer, A.P., 1996. Export flux of carbon at the equator during the EqPac time-series cruises estimated from ^{234}Th measurements. Deep-Sea Research II 43, 1133–1154.

Benitez-Nelson, C., Buesseler, K.O., Rutgers van der Loeff, M., Andrews, J., Ball, L., Crossin, G., Charette, M., 2000. Testing a new small-volume technique for determining thorium-234 in seawater. Journal of Radioanalytical and Nuclear Chemistry (submitted for publication).

Bidigare, R.R., Hanson, K.L., Buesseler, K.O., Wakeham, S.G., Freeman, K.H., Pancost, R.D., Millero, F.J., Steinberg, P., Popp, B.N., Latasa, M., Landry, M.R., Laws, E.A., 1999. Iron-stimulated changes in ^{13}C fractionation and export by equatorial Pacific phytoplankton. Paleoceanography 14 (5), 589–595.

Brown, S.L., Landry, M.R., 2000. Microbial community structure and biomass at the peak of a Polar Front summer bloom along 170°0 W. Deep-Sea Research II (submitted for publication).

Brzezinski, M.A., 1985. The Si:C:N ratio of marine diatoms. Marine Biology Berlin 21, 347–357.

Brzezinski, M.A., Nelson, D.M., 1986. A solvent extraction method for the colorimetric determination of nanomolar concentrations of silicic acid in seawater. Marine Chemistry 19, 139–151.

Brzezinski, M.A., Nelson, Franck, V.M. Sigmon, D.E., 2000a. Silicon dynamics within an intense open-ocean diatom bloom in the Pacific sector of the Southern Ocean. Deep-Sea Research II (submitted for publication).

Brzezinski, M.A., Dickson, M.-L., Nelson, D.M., Sambrotto, R., 2000b. Ratios of Si, C and N uptake by microplankton in the low Fe waters of the Southern Ocean. Limnology and Oceanography (submitted for publication).

Buesseler, K.O., 1998. The de-coupling of production and particulate export in the surface ocean. Global Biogoechemical Cycles 12 (2), 297–310.

Buesseler, K.O., Bacon, M.P., Cochran, J.K., Livingston, H.D., 1992. Carbon and nitrogen export during the JGOFS North Atlantic Bloom experiment estimated from ^{234}Th:^{238}U disequilibria. Deep-Sea Research II 39 (7/8), 1115–1137.

Buesseler, K.O., Andrews, J.A., Hartman, M.C., Belastock, R., Chai, F., 1995. Regional estimates of the export flux of particulate organic carbon derived from thorium-234 during the JGOFS EQPAC program. Deep-Sea Research II 42 (2–3), 777–804.

Buesseler, K.O., Ball, L., Andrews, J., Benitez-Nelson, C., Belastock, R., Chai, F., Chao, Y., 1998. Upper ocean export of particulate organic carbon in the Arabian Sea derived from thorium 234. Deep-Sea Research II 45 (10-11), 2461–2487.

Buesseler, K.O., Steinberg, D.K., Michaels, A.F., Johnson, R.J., Andrews, J.E., Valdes, J.R., Price, J.F., 2000a. A comparison of the quantity and quality of material caught in a neutrally buoyant versus surface-tethered sediment trap. Deep-Sea Research I 47, 277–294.

Buesseler, K.O., Benitez-Nelson, C., Rutgers van der Loeff, M., Andrews, J., Ball, L., Crossin, G., Charette, M., 2000b. An intercomparison of small- and large-volume techniques for thorium-234 in seawater. Marine Chemistry, in press.

Charette, M.A., Buesseler, K.O., 2000. Delay in the onset of particle export during an iron fertilization experiment in the Southern Ocean. Geochemistry, Geophysics, Geosystems, in press.

Charette, M.A., Moran, S.B., Bishop, J.K.B., 1999. ^{234}Th as a tracer of particulate organic carbon export in the subarctic Northeast Pacific Ocean. Deep-Sea Research II 46, 2833–2861.

Chen, J.H., Edwards, R.L., Wasserburg, G.J., 1986. ^{238}U, ^{234}U and ^{232}Th in seawater. Earth and Planetary Science Letters 80, 241–251.

Coale, K.H., Bruland, K.W., 1987. Oceanic stratified euphotic zone as elucidated by ^{234}Th:^{238}U disequilibria. Limnology and Oceanography 32 (1), 189–200.

Cochran, J.K., Barnes, C., Achman, D., Hirschberg, D.J., 1995. Thorium-234/uranium-238 disequilibrium as an indicator of scavenging rates and particulate organic carbon fluxes in the Northeast Water Polynya, Greenland. Journal of Geophysical Research 100 (C3), 4399–4410.

Cochran, J.K., Roberts, K.A., Barnes, C., Achman, D., 1997. Radionuclides as indicators of particle and carbon dynamics on the East Greenland Shelf. Radioprotection-colloques 32 (C2). In: Germain, P., Guary, J.C., Guegueniat, P., Metivier, H (Eds.), Proceedings of RADOC 96-97 ''Radionuclides in the Oceans'', pp. 129–136.

Cochran, J.K, Buesseler, K.O., Bacon, M.P., Wang, H.W., Hirschberg, D.J., Ball, L., Andrews, J., Crossin, G., Fleer, A., 2000. Short-lived thorium isotopes (^{234}Th, ^{228}Th) as indicators of POC export and particle cycling in the Ross Sea, Southern Ocean. Deep-Sea Research II (submitted for publication).

DeMaster, D.J., 1981. The supply and accumulation of silica in the marine environment. Geochimica Cosmochimica Acta 45, 1715–1732.

DeMaster, D.J., Nelson, T.M., Harden, S.L., Nittrouer, C.A., 1991. The cycling and accumulation of biogenic silica and organic carbon in Antarctic deep-sea and continental margin environments. Marine Chemistry 35, 489–502.

DeMaster, D.J., Ragueneau, O., Nittrouer, C.A., 1996. Preservation efficiencies and accumulation rates for biogenic silica and organic C, N, and P in high latitude sediments: the Ross Sea. Journal of Geophysical Research 101, 18501–18518.

Dugdale, R.C., Wilkerson, F.P., Minas, H.J., 1995. The role of the silicate pump in driving new production. Deep-Sea Research I 42, 697–719.

Dunne, J.P., Murray, J.W., 1999. Sensitivity of ^{234}Th export to physical processes in the central equatorial Pacific. Deep-Sea Research I 46, 831–854.

Gustafsson, Ö., Buesseler, K.O., Geyer, W.R., Moran, S.B., Gschwend, P.M., 1998. On the relative significance of horizontal and vertical transport of chemicals in the coastal ocean: application of a two-dimensional Th-234 cycling model. Continental Shelf Research 18, 805–829.

Hartman, M.C. Buesseler, K.O., 1994. Adsorbers for in-situ collection and at-sea gamma analysis of dissolved thorium-234 in seawater. WHOI Technical Report, WHOI-94-15.

Hiscock, M.R., Marra, J., Smith, W.O., Barber, R.T., 2000. Primary production and its regulation in the Antarctic Polar Front Zone in 1997 and 1998. EOS 80 (40), OS265.

Honjo, S., Francois, R., Manganini, S., Dymond, J., Collier, R., 2000. Export fluxes in the western Pacific sector of the Southern Ocean along 170°W. Deep-Sea Research II (submitted for publication).

Hutchins, D.A., Bruland, K.W., 1998. Iron-limited diatom growth and Si:N uptake ratios in a coastal upwelling regime. Nature 393, 561–564.

Kumar, N., Anderson, R.F., Mortlock, R.A., Froelich, P.N., Kublik, P., Dittrich-Hannen, B., Suter, M., 1995. Increased biological productivity and export production in the glacial Southern Ocean. Nature 378, 675–680.

Langone, L., Frignani, M., Cochran, J.K., Ravaioli, M., 1997. Scavenging processes and export fluxes close to a retreating seasonal ice margin, Ross Sea, Antarctica. Water, Air and Soil Pollution 99, 705–715.

Livingston, H.D., Cochran, J.K., 1987. Determination of transuranic and thorium isotopes in ocean water: in solution and in filterable particles. Journal of Radioanalytical and Nuclear Chemistry, Articles 115 (2), 299–308.

Measures, C. I., Vink, S., 2000. Dissolved Fe in the upper waters of the Southern Ocean during the 1997/98 US JGOFS cruises. Deep-Sea Research II (submitted for publication).

Moore, J.K., Abbott, M.R., Richman, J.G., Smith, W.O., Cowles, T.J., Coale, K.H., Gardner, W.D., Barber, R.T., 1999. SeaWiFS satellite ocean color data from the Southern Ocean. Geophysical Research Letters 26 (10), 1465–1468.

Moran, S.B., Buesseler, K.O., 1993. Size-fractionated ^{234}Th in continental shelf waters off New England: implications for the role of colloids in oceanic trace metal scavenging. Journal of Marine Research 51, 893–922.

Moran, S.B., Smith, J.N., 2000. ^{234}Th as a tracer of scavenging and particle export in the Beaufort Sea. Continental Shelf Research 20, 153–167.

Moran, S.B., Charette, M.A., Pike, S.M., Wicklund, C.A., 1999. Differences in seawater particulate organic carbon concentration in samples collected using small-volume and large-volume methods: the importance of DOC adsorption to the filter blank. Marine Chemistry 67, 33–42.

Mortlock, R.A., Charles, C.D., Froelich, P.N., Zibello, M.A., Saltzmann, J., Hayes, J.D., Burckle, L.H., 1991. Evidence for lower productivity in the Antarctic Ocean during the last glaciation. Nature 351, 220–223.

Murray, J.W., Young, J., Newton, J., Dunne, J., Chapin, T., Paul, B., 1996. Export flux of particulate organic carbon from the central equatorial Pacific determined using a combined drifting trap-^{234}Th approach. Deep-Sea Research II 43, 1095–1132.

Nelson, D.M., Treguer, P., Brzezinski, M.A., Leynaiert, A., Queguiner, B., 1995. Production and resolution of biogenic silica in the ocean: revised global estimates, comparisons with regional data and relationship to biogenic sedimentation. Global Biogeochemical Cycles 9, 359–372.

Orsi, A.H., Whitworth, T. III, Nowlin, W.D., Jr., 1995. On the meridional extent and fronts of the Antarctic Circumpolar Current. Deep-Sea Research I 42(5), 641–673.

Pondaven, P., Ragueneau, O., Treguer, P., Hauvespre, A., Dezileau, Reyss, J.L., 2000. Resolving the "opal paradox" in the Southern Ocean. Nature 405, 168–172.

Queguiner, B., Treguer, P., Peeken, I., Scharek, R., 1997. Biogeochemical dynamics of the silicon cycle in the Atlantic sector of the Southern Ocean during the austral spring 1992. Deep-Sea Research II 44 (1–2), 69–90.

Rutgers van der Loeff, M.M., Friedrich, J., Bathmann, U.V, 1997. Carbon export during the spring bloom at the Southern Polar Front, determined with the natural tracer ^{234}Th. Deep-Sea Research II 44 (1–2), 457–478.

Rutgers van der Loeff, M.M., Buesseler, K., Bathmann, U., Hense, I., Andrews, J., 2000. Steady summer production and a sudden spring bloom make a comparable contribution to carbon and opal export near the Antarctic Polar Front, SE Atlantic. Deep-Sea Research II (submitted for publication).

Sarmiento, J.L., Toggweiler, R., 1984. A new model for the role of the oceans in determining atmospheric pCO_2. Nature 308, 621–624.

Scholten, J.C., Fietzke, J., Vogler, S., Rutgers van der Loeff, M., Mangini, A., Koeve, W., Stoffers, P., Antia, A., Neuer, S., Waniek, J., 2000. Trapping efficiencies of sediment traps from the deep eastern North Atlantic: The ^{230}Th calibration. JGOFS North Atlantic synthesis. Deep-Sea Research II: in press.

Shimmield, G.B., Ritchie, G.R., 1995. The impact of marginal ice zone processes on the distribution of ^{210}Pb, ^{210}Po and ^{234}Th and implications for new production in the Bellingshausen sea, Antarctica. Deep-Sea Research II 42 (4–5), 1313–1335.

Sigmon, D.E., Nelson, D.M., Brzezinski, M.A., 2000. Biological control of the surface layer silicon cycle in the Southern Ocean. Deep-Sea Research II (in preparation).

Smith, W.O., Anderson, R.F., Moore, J.K., Codispoti, L.A., Morrison, J.M., 2000. The US Southern Ocean Joint Global Ocean Flux Study: An introduction to AESOPS. Deep-Sea Research II (submitted for publication).

Strickland, J.D.H., Parsons, T.R., 1972. A Practical Handbook of Seawater Analysis. Fisheries Research Board of Canada, 310p.

Tanaka, N., Takeda, Y., Tsunogai, S., 1983. Biological effect on removal of Th-234, Po-210 and Pb-210 from surface water in Funka Bay, Japan. Geochimica Cosmochimica Acta 47, 1783–1790.

Treguer, P., Nelson, D.M., Van Bennekom, A.J., DeMaster, D.J., Leynaert, A., Queguiner, B., 1995. The silica balance in the world ocean: a reestimate. Science 268 (5209), 375–379.

Wei, C.-L., Murray, J.W., 1991. ^{234}Th/^{238}U disequilibria in the Black Sea. Deep-Sea Research 38 (2), S855–S873.

Yu, E.-F., Francois, R., Bacon, M.P., Honjo, S., Fleer, A.P., Manganini, S.J., Rutgers van der Loeff, M.M., Ittekot, V., 2000. Trapping efficiency of bottom-tethered sediment traps estimated from the intercepted fluxes of ^{230}Th and ^{231}Pa. Deep-Sea Research I (in press).